Inversion of forest canopy height in south of China by integrating GLAS and MERSI: The case of Jiangxi province in China

DONG Lixin[1,2], LI Guicai[1,2], TANG Shihao[1,2]

1. *Key Laboratory of Radiometric Calibration and Validation for Environmental Satellites*, *Beijing* 100081, *China*;
2. *National Satellite Meteorological Center*, *Beijing* 100081, *China*

Abstract: For inversion of forest canopy height in large scale, it is of great significance to integrate space-borne Lidar and optical remote sensing data effectively. The homemade satellite will provide a plentiful datum for forest ecological researches. In this paper, the processing of GLAS waveform data and the algorithm of forest canopy height in different terrain were implemented. The GLAS + MERSI joint inversion model of canopy height of different forest types in regional scale was established and used to map the forest canopy height of Jiangxi province. Overall, high accuracy was observed for the canopy height estimated by GLAS + MERSI joint inversion model with R^2=0.733 for the needle-leaf forest, following by the broadleaf forest (R^2=0.610). The results showed that the established model was workable. It was found that the GLAS + MERSI joint inversion model which considers the optical remote sensing of biophysical parameters can provide good estimates of forest canopy height at regional scale. The space distribution characteristic was found consistent with the data of land cover.

Key words: forest canopy height, Lidar, GLAS, FY3A-MERSI

CLC number: TP79 **Document code**: A

Citation format: Dong L X, Li G C and Tang S H. 2011. Inversion of forest canopy height in south of China by integrating GLAS and MERSI: The case of Jiangxi province in China. *Journal of Remote Sensing*, **15**(6): 1301–1314

1 INTRODUCTION

Forest vertical structure (height, leaf area index (LAI) *etc*.) and biomass are the sensitive parameters in the carbon cycle studies. The traditional methods of forest parameters measurement have some limitations in large scale. However, due to the direct measurement capability with high precision on the forest vertical structure, Lidar technology shows unsurpassed advantages in the measurement of forestry ecological parameters.

In recent years, many researches (Nilson, 1996; Means, *et al*., 1999; Lefsky, *et al*., 1997, 1999, 2002, 2005; Hudak, *et al*., 2002; Hyde. *et al*., 2005) have developed some Lidar's algorithms for the estimation of forest parameters. These studies greatly promote the Lidar applications in forestry ecological fields. Vegetation Canopy LIDAR (VCL) system program has already been proposed by NASA-GSFC and the university of Maryland. Many experiments have been conducted in US, Canada and Australia. The vertical structure and fraction of coverage of the temperate and tropical forests have been successful inversed in these experiments. Sun and Ranson (2000) found that laser wave can well reflect forest vertical structure by integrating the forest growth model and the wave simulation model. Lefsky, *et al*. (1997) developed an artificial means to testing the ground wave for estimation of the tree height. Hyde, *et al*. (2005) developed an automated testing strategy of the ground and crown waves, which greatly enhanced the laser application prospect in canopy height measurement.

In China, Pang, *et al*. (2006a, 2007) provided the theoretical simulation on the complete waveforms of the big footprint Lidar system. Sun, *et al*. (2008) made the evaluation on the Icesat-GLAS land data. Dong (2008) proposed a centroid-terrain index algorithm by modifying the terrain index algorithm (Lefsky, *et al*., 1997) and applied it into the research of forest canopy height and biomass in the steeply sloping areas.

Due to discrete items for Lidar data, it is needed to combine grid remote sensing data for inversion of the forest parameters in regional scale. Lefsky, *et al*. (2001) pointed out that in spite of the laser radar being sample data, it will greatly enhance the forestry measurement by integrating other grid remote sensing data owing to the very high precision. At present, combining Lidar data with optical, multi-angular and microwave remote sensing data is an effective inversion way of canopy height and biomass in regional scale (Sun, *et al*., 2000; Pang, *et al*., 2006b, 2008; Dong, *et al*., 2009).

Received: 2010-07-26; **Accepted:** 2011-03-22

Foundation: The National Basic Research Program (973 Program) (No. 2010CB950701-01); Climate change special project (No. CCSF-09-09)

First author biography: DONG Lixin(1973—), male, Ph.D., associate professor. His research interest is Lidar theory and applications. E-mail: dlx_water@163.com

In this study, the mainly forest reserves in Jiangxi province in south of China was selected as the experimental area and the field survey was conducted in October 2009. Based on the processing of the wave data at GLAS foot and the algorithm of canopy height in different terrains, the forest canopy height on GLAS foot were inversed successfully. And the forest canopy height of different types in regional scale was also inversed by the joint inversion model combining GLAS and FY3A/MERSI data. The forest canopy height in Jiangxi province has been mapped.

2 STUDY AREA AND DATA

2.1 Study Area

Jiangxi province is one of the main regions of forest reserves in the middle and lower reaches of Yangtse River. It is located in 113º58′E—118º48′E, 24º48′N—30º07′N, and covers an area of approximately 16.69×10^4 km^2. The altitude is about 300—600 m. It belongs to mid-subtropical and subtropical zone forest ecosystems. There are about 36 natural forest ecosystems reserves. Its total area is approximately 2.13×10^5 ha. The forest vegetation is mainly classified into five types: Subtropical and Tropical evergreen broad-leaved forest, Temperate Zone deciduous broad-leaved forest, Frigid Zone coniferous forest and mingled forests and shrubbery. Most of the forest is the natural secondary forest and the coverage rate of forest is about 60.05%. The vertical distribution character of forest vegetation in hilly and mountain regions is obvious. The vertical distribution regularity from low to high altitude is as follows: moso bamboo, evergreen broad-leaved forest, coniferous and broad-leaved mingled forests, coniferous forests, montane moss elfin forest, and alpine bush meadow. The main landscape type is mountain and hills, and mountainous area accounts for 36%, the hilly area accounts for 42%, plain and hummock (include waters) accounts for the remain 22%.

2.2 Data

2.2.1 GLAS data

The scientific and testing satellite of the United States called ICESat was launched on 2003-01-12. It was a spaceborne, waveform sampling Lidar satellite which is used for measuring and monitoring ice sheet and land topography as well as cloud, atmospheric, and vegetation properties. The Geo-science Laser Altimeter System (GLAS) instrument on aboard ICESat with three laser instruments performs the observation mission with 91 d repetitive orbital scheme (every 33 d). The distance between two adjacent orbital was 15 km near the equator and 2.5 km in 80°N. For maximum covering the polar region, the different periods of time in every year were chosen. The laser spot diameter was 70 m and the intervals distance between two spots was 175 m (Brenner, *et al*., 2002). It provides value sample data of the vegetation height with high vertical resolution. The waveforms with vegetation vertical structure information in 1064 nm waveband will be able to evaluate the vegetation and biomass distribution better (Zwally, *et al*., 2002).

In this study, GLA01 and GLA14 data from L3F (May—June, 2008) were used. GLAS data in study areas was shown in Fig. 1. The field sample area of LAI and foundation Lidar were shown in lower right small figure.

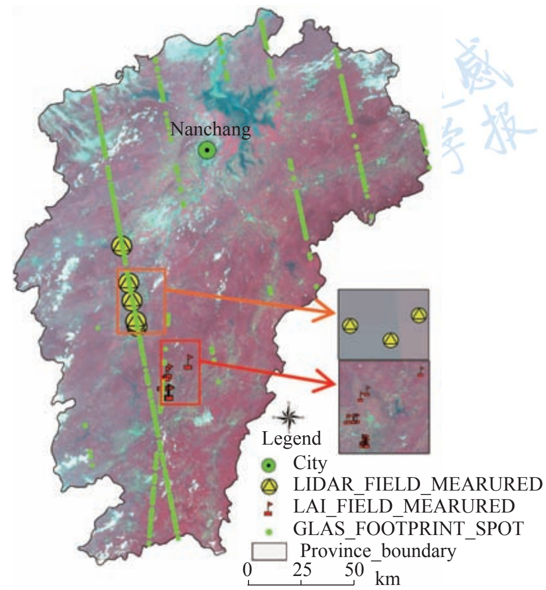

Fig. 1 MERSI+GLAS data and distribution of field sample area in Jiangxi province

2.2.2 FY3A-MERSI data

FengYun-3 (FY-3) was the second generation polar-orbiting meteorological satellite series of China. The first satellite named FY-3A of this series was launched on 2008-05-27. The new generation satellites series were to provide three-dimensional, quantitative, multi-spectrum global remote sensing data under all weather conditions, which will greatly help the operational numerical weather prediction, global change research, climate diagnostics and prediction, and natural disasters monitoring (Yang, *et al*., 2009). Observations from all of the 11 instruments on aboard this satellite were broadcast on L and X bands. Meanwhile, FY-3A Medium Resolution Spectral Imager (MERSI) was similar with MODIS in spatial resolutions (0.25—1.0 km). And there were five channels with 250 m resolution from visible-infrared bands. In this paper, the MERSI data with a few clouds (<2%) on 2009-08-29 in Jiangxi province were obtained. The wavelength of the data was between 0.47—0.865 um. Many pre-processing such as geographical corrections, cloud detection, atmospheric correction, and projective transformation were accomplished (Fig. 1).

2.2.3 Field experiment data

Five sample areas of GLAS footprint in plant area of Jiangxi province were selected. Due to the foundations lidar instrument was heavily and hard to taken, these sample sites were all near the roads. Measurement was accomplished in three different directions (every 120°) in the 70 m Lidar footprint (In the small figure in Fig. 1). Lidar point clouds data were obtained by the foundations laser radar scanning instrument (Riegl LMS-Z360i), and the maximum tree height were extracted by the Lidar software for validation. Under given conditions, the scanning scope of the foundations Lidar was 200 m radius, which matching with GLAS spot size. So, theses data can be used to validate the inversion results of GLAS. Moreover, other sample areas with three 10 m×10 m sample sites were set up along GLAS foot. And many trees parameters measured by traditional methods in these sample sites were used chiefly for the coefficients fitting of the algorithm. LAI data of different density forest were obtained from the field data measured by Luo, *et al*. (2005) in Xinguo County. In addition, DEM was used to the terrain index calculation.

3 ALGORITHM AND MODEL

3.1 Algorithm of forest canopy height in GLAS footprint

Firstly, we process the Lidar return waveforms data in GLAS footprint (Sun, *et al*., 2008; Dong, *et al*., 2008; Duncanson, *et al*., 2010). The algorithm was mainly composed of the following steps: extraction of valid waveforms, gauss filtering, noise estimation, and gauss wave decomposition and fitting, signal beginning and end position detection, ground wave position detection and results correction.

After extracting valid waveforms data, smoothing filtering was realized by using a gauss filter which width was the same as the laser pulse width (4 ns). The background noises in the beginning and end of phase were estimated using the histogram method (Sun, *et al*., 2008) and the features parameters (mean value and standard deviations) were also calculated. Then the waveform was fitted effectively by Levenberg Marquardt nonlinear method, and the wave peak position of the ground and forest canopy was determined by gauss wave decomposition (Dong, 2008). The algorithm parameters were illustrated in Fig. 2.

The beginning and end positions of GLAS wave peak can be detected using the features parameters through repeated attempts. If the value was greater than $threshold_{start}$(Eq. (1) and Eq. (2)), it was the beginning position. If the value was lower than $threshold_{end}$, it was the end position.

$$threshold_{start}=meanns_{start}+4\times sdevns_{start} \tag{1}$$

$$threshold_{end}=meanns_{end}+4\times sdevns_{end} \tag{2}$$

Finally, the detection method of ground wave peak position was to search adversely from the end signal. If the distance between the mainly waves peak position and the end signal was larger than a half wide of the laser pulse, the wave peak was ground wave peak.

(1) Algorithm and correction of forest canopy height in gently areas

The return wave length (*Range*) can be calculated from the position of forest canopy and ground wave peak. The canopy height (*H*) was the product of *Range* and record interval size (*BinSize*), namely,

$$H=Range\times BinSize \tag{3}$$

In order to overcome the problem of the broadened of ground wave and the forward broadened of first wave in gentle slope and

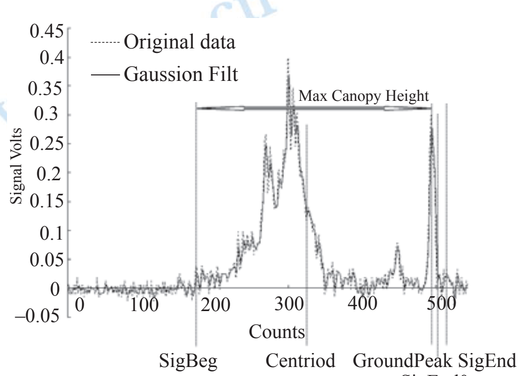

Fig. 2 Illustration of GLAS waveform parameters

relatively large roughness areas, the results need to be corrected by the method of using the distance between *SigEnd0* and *SigEnd* (Sun, *et al*., 2008). The correction result (H_t) is,

$$H_t=H-(SigEnd-SigEnd0) \tag{4}$$

The end wave expanded from *SigEnd*0 to *SigEnd* because of the impact of terrain; *SigEnd*0 was the ground wave position plus the half wide of the laser pulse.

(2) Model of forest canopy height in grater slope areas

Studies show that grater slope can impact greatly on the big footprint Lidar return wave (Harding, *et al*., 1994; Heyder, 2005), leading to difficulty in extracting the tree height from the waveform directly in grater slope areas. The centroid-terrain index algorithm has better inversion accuracy of forest canopy height in the grater slope areas (Dong, 2008) with the following formula,

$$H=a_0(w_c-a_1\times g+a_2 l) \tag{5}$$

where w_c is the distance between the centroid and the end wave, the centroid is the position of half of waveforms area, g is terrain index in unit of m, l is leading edge of waveform, with unit of m, a_0, a_1, a_2 are all coefficients.

3.2 Calculation of MERSI LAI and Fcover

Taking MERSI vegetation indices (NDVI) as independent variable, the field measured LAI as dependent variable, the relation model between LAI and NDVI has been established (Eq. (6)).

$$\text{LAI} = a\times\ln(\text{NDVI})+ b \tag{6}$$

Fraction of forest coverage (Fc) was evaluated using a model 'pixel bipartition'.

$$\text{Fc} = \frac{\text{NDVI}-\text{NDVI}_{min}}{\text{NDVI}_{max}-\text{NDVI}_{min}} \tag{7}$$

The validation results of LAI and Fc can be used in the inversion of forest canopy height in regional scale.

3.3 GLAS+MERSI joint model of forest canopy height in regional scale

For most of plants, the leaf area increases with the plant height during the vegetation growth. For different species and varieties of crops, the relationships of conversion between crop height (*H*), fraction of coverage (Fc) and LAI was proposed by Zhang (1996).

$$H = A_H\frac{\text{LAI}}{\text{Fc}} \tag{8}$$

where *H* was the plant height; LAI was leaf area index; Fc was the fraction of coverage; A_H was the coefficients.

In the forestry ecological study fields, the allometric method using of the relationship between LAI and the surveyed factors (plant height and stem diameter) was one of the traditional measurements method between biomass and LAI. On basic theories, stem and branches were the collection of the nutrition tube supporting leaves (Chen, *et al*., 1997; Dantec, *et al*., 2000). Studies showed that height and canopy diameter can reflect the structure characteristics of vegetation better, consequently, the inversion model of LAI and aboveground biomass was established intuitively (Jiang & Lu, 1982; Hou, *et al*., 1994).

In conclusion, the study of correlation between forest height, LAI and coverage can provide a theoretical basis and reasonable physical and biological meanings for the space extrapolation of forests canopy height.

4 RESULT VALIDATION AND ANALYSIS

4.1 MERSI-LAI and coverage results

Using the field surveyed LAI and MERSI NDVI data, the relational models between LAI and MERSI-NDVI in different density forest were established. As shown in Table 1, the value of R^2 in dense forest was 0.8597. R^2 of middle density forest ($0.8 > Fc > 0.4$) was 0.6485. R^2 of sparse forest was only 0.3538. Hence, a fairly good correlation existed between LAI and NDVI and it can be used for LAI calculation. It can be seen from Fig. 3 that the value of LAI in the southeastern regions of Jiangxi province and around forest regions of Qianyanzhou ecological experimental and research station were the highest.

Table 1 Relationship between LAI and MERSI-NDVI in different density forests

Density	Relationship Model	R^2	Sample number
Dense	LAI=5.4774×ln(NDVI) + 6.8523	0. 860	8
Middle	LAI=2.1817×ln(NDVI) + 3.1055	0. 649	5
Sparse	LAI=1.9201×ln(NDVI) + 2.7168	0.354	10

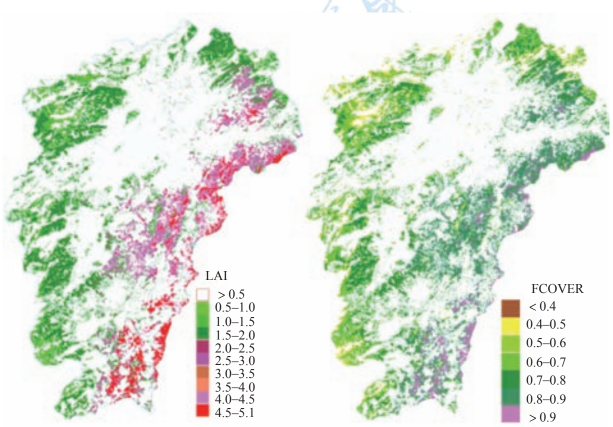

Fig. 3 Distribution of LAI and coverage of forest in Jiangxi province

The range of MERSI-LAI in different density forest was different. Statistical analysis on 250 m LAI characteristics derived from MERSI data found that the value of LAI of needle-leaf forests ranged from 0.5 to 5.2. And histogram analysis found that the ratio of LAI ranged from 1 to 5.1 was 96.11%. By contrast, our results were consistent with the measurement results (1.0—4.0) of Luo, *et al*. (2002) and Zhang, *et al*. (2003). Spatial distribution of LAI was relatively reasonable.

Compare with MODIS LAI product after MERSI LAI results were expanded to 1 km resolution, the spatial distribution was basically consistent between the two models. The absolute difference of LAI in coniferous forests and broad-leaved forest was within 1. That of mixed forest was largest because of the error of MODIS LAI products and the worse relationship between LAI and NDVI in mixed forest.

Through the forest coverage map, it can be seen that the inversion result of forest coverage was consistent with the vegetation distribution in Jiangxi province. Fitted with the measured coverage data, the value of R^2 was 0.8, and the error with sample data was about 0.05 to −0.05. In addition, compared to the measured results by Sheng (2001) , which the forest coverage value in sample area of Shangcun wood farm was 0.74, the difference value with the inversion results of forest coverage (0.769) was only 0.029.

As a whole, the inversion results of LAI and forest coverage derived from 250 m MERSI data was more satisfactory and can be used to subsequent calculation.

4.2 ‘Satellite-ground’ validation of forest canopy height in GLAS footprint

The forest canopy height in GLAS footprint in Jiangxi province was demonstrated in Fig. 4.

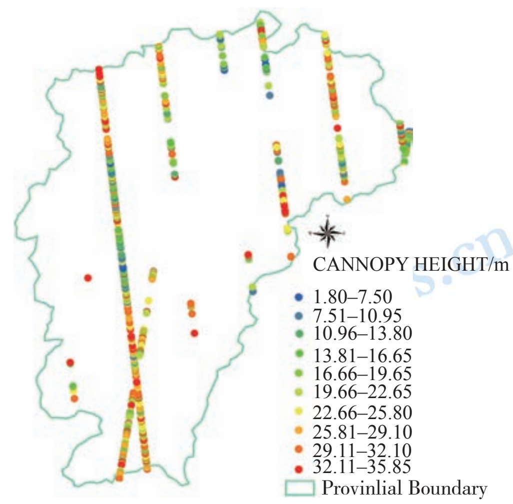

Fig. 4 Results of forest canopy height in GLAS footprint

Compared with the forest distribution map, it was found that the results were well consistent with the vegetation distribution of study area. The forest regions with heights above 20 m were mainly located in the northeast, northwest and southern of Jiangxi province. This was well consistent with the forest biomass distribution. Moreover, the value of vegetation height in the farmland and grassland regions was much lower.

In order to verify the accuracy of the forest canopy height extracted by GLAS waveform data, and to reduce the inaccuracy of manual estimation, the inversion results of forest canopy height were compared with the measured results by the ground laser radar instrument (Fig. 5).

From Fig. 5, except for the largest error of forest canopy height of sample sites 4, probably due to the large slopes ranged from 20° to 25°, the precision of other results were reasonably good. By comparing three kinds of measurement technologies, it can be found that the inversion results of GLAS represents well the maximum height of sample area; the results measured by the ground laser radar are different from the position of sample site; the results measured by manual estimation are most uncertain. Because the ground laser radar was heavy, and great volume and the processing of Lidar clouds data were time-consuming, it was difficult to measure more sample regions. Therefore, these sample areas matching

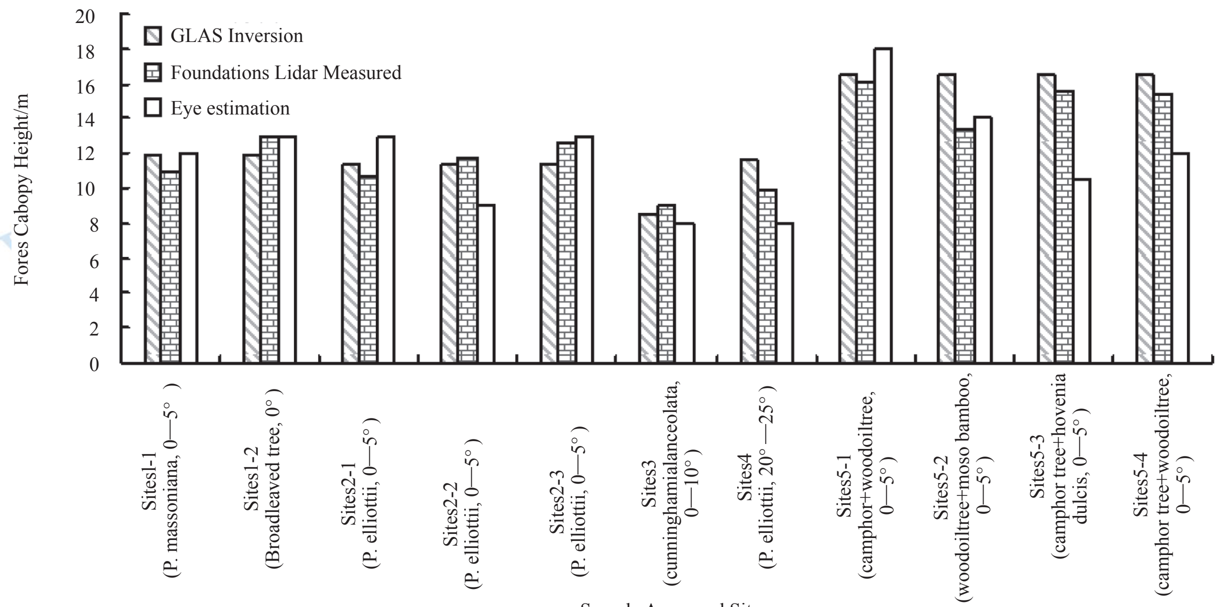

Fig. 5 'Satellite-ground' validation of the results of forest canopy heigh

exactly with GLAS footprint were only measured.

On the whole, the inversion results of forest canopy height in GLAS footprint in Jiangxi province were satisfactory and can be used for the inversion of forest canopy height in regional scale.

4.3 Forest canopy height in regional scale

The GLAS + MERSI joint inversion model of canopy height in different forest types were established based on the relationship between the height and ratio of LAI and Fc (Table 2). Because the relationship between LAI and NDVI in sparse forest was relatively poor, its model was not including in Table 2.

Table 2 The GLAS + MERSI joint inversion model of canopy height in different forest types

Type / Density		Joint inversion model	R^2	Sample number
Needle-leaved	Dense	*HEIGHT*= −595.9×ln(LAI/Fc)+989.44	0.792	5
	Middle	*HEIGHT*=307.37×ln(LAI/Fc) −242.23	0.733	7
Broad-leaved	Dense	*HEIGHT*=288.13×ln(LAI/Fc) −443.51	0.616	7
	Middle	*HEIGHT*=22.494×ln(LAI/Fc)+7.3312	0.610	7
Mixed forest	Dense	*HEIGHT*=673.09×ln(LAI/Fc) −1064.1	0.413	39
	Middle	*HEIGHT*=214.63×ln(LAI/Fc) −163.16	0.407	59

Notes: *HEIGHT* was forest canopy height; LAI and Fc were leaf area index and coverage from MERSI data, respectively

From Table 2, the joint inversion model of Needle-leaf forest was best, with R^2 higher than 0.733. Broad-leaved forest was the second, with R^2 around 0.61. They all reached 0.01 significant levels by the means of *T*-test. The joint model of mixed forest was relatively poor. It might be relative to the physical properties of the LAI and coverage of mixed forest.

The distribution of forest canopy height in study area was accomplished using above joint inversion model. Forest canopy height of study area in regional scale was shown in Fig. 6, and the white area was none-forest areas. In order to further evaluating the accuracy, the results were compared with the forest type distribution map derived from Landsat TM data and found it was consistent with the forest type distribution in study area. Specifically, it was obvious that higher value regions of canopy height were located in Wuyi Mountain branch range of the southern and some forest reserves regions. The forest canopy height in Jinggang and Lu Mountain were also relatively high. This was consistent with the distribution of forest biomass and the results of forest canopy height in GLAS footprint. Further verification work will be continued.

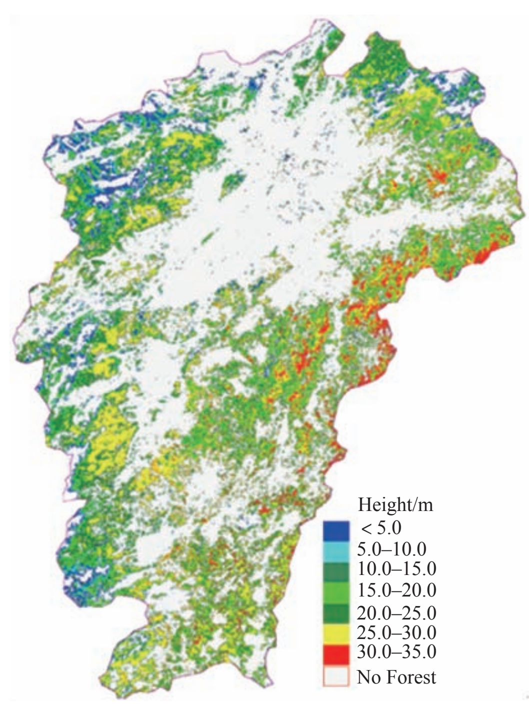

Fig. 6 Results of forest canopy height with GLAS + MERSI joint inversion model

5 CONCLUSION AND DISCUSSION

Algorithmic of GLAS data processing and inversion models of forest canopy height in different terrain conditions were detailed described in this paper. Specially, the joint inversion model integrating GLAS and FY3A-MERSI data was discussed.

(1) The results of forest canopy height on different terrain conditions show good accuracy. The 'centroid-terrain index' method has a wide application prospect in grater slope terrain.

(2) Precision of LAI derived from FY3A-MERSI data was good and satisfied. The relationship between forest canopy height and the ratio of LAI and Fc were relatively better. FY3A-MERSI data was an ideal optical data because of its better availability.

(3) As spatial distribution patterns were concerned, the results of forest canopy height by GLAS+MERSI joint inversion model was consistent with the distribution of forest type map. Hence, these results can be better applied to the quantitative inversion of other forest biophysics parameters.

Acknowledgements: Thanks for the help in ground Lidar (Rieg1 LMS- Z360i) using from Doctor Huang H.B.; Thanks the members' works in the experiment of the ground Lidar measurement in Jiangxi province.

REFERENCES

Brenner A C, Jay Zwally H, Bentley C R, Bea M C, David J H, Michelle A H, Minster J B, Lee Anne R, Saba J L, Thomas R H and Yi D H. 2000. Derivation of range and range distributions from laser pulse waveform analysis for surface elevations, roughness, slope, and vegetation heights. GLAS Algorithm Theoretical Basis Document Version 310

Chen J M, Rich P M, Gower S T, Norman J M and Plummer S. 1997. Leaf area index of boreal forests: theory, techniques and measurements. *Journal of Geophysical Research*, **102**(D24): 29429–29443

Dong L X. 2008. Estimation of the Forest Canopy Height and Aboveground Biomass Based on Multiplicatel Remote Sensing in Three Gorges. Beijing: Institute of Remote Sensing Applications Chinese Academy of Sciences (CAS): 56–98

Dong L X, Wu B F and Guo Z H. 2009. Estimation of forest canopy height by integrating multisensor data. *Proceedings of the SPIE*, **7471**: 74710H,.DOI: 10.1117/12.836304

Duncanson L I, Niemann K O and Wulder M A. 2010. Estimating forest canopy height and terrain relief from GLAS waveform metrics. *Remote Sensing of Environment*, **114**(1): 138–154

Harding D J, Bufton J L and Frawley J J. 1994. Satellite laser altimetry of terrestrial topography: vertical accuracy as a function of surface slope, roughness, and cloud cover. *IEEE Transactions on Geoscience and Remote Sensing*, **32**(2): 329-339 DOI: 10.1109/36.295048

Heyder U. 2005. Vertical Forest Structure from ICESat/GLAS Lidar Data. Masters thesis Geography, VCL.12–50

Hou P, Yi L K and Yan C. 1994. Study on biomass of ammopipyanthus. *Arid Zone Research*, **11**(2): 16–18

Hudak A T, Lefsky M A, Cohen W B and Berterretche M. 2002. Integration of lidar and Landsat ETM+ data for estimating and mapping forest canopy height. *Remote Sensing of Environment*, **82**(2-3): 397–416 DOI: 10.1016/S0034-4257(02)00056-1

Hyde P, Dubayah R, Peterson B, Blair J B, Hofton M, Hunsaker C, Knox R and Walker W. 2005. Mapping forest structure for wildlife habitat analysis using waveform lidar: validation of montane ecosystems. *Remote Sensing of Environment*, **96**(3–4): 427–437 DOI: 10.1016/j.rse.2005.03.005

Jiang F Q and Lu F Y. 1982. The model of estimating above-ground biomass of caragana microphylla brush. *Acta Ecologica Sinica*, **2**(2):103–108

Le Dantec V, DufreÃne E and Saugier B. 2000. Interannual and spatial variation in maximum leaf area index of temperate deciduous stands. *Forest Ecology and Management*, **134**: 71–81 DOI: 10.1016/S0378-1127(99)00246-7

Lefsky M A, Cohen W B, Acker S A, Spies T A, Parker G G and Harding D. 1997. Lidar remote sensing of forest canopy structure and related biophysical parameters at the H.J. Andrews experimental forest, Oregon, USA//Greer J D, ed. Natural Resources Management using Remote Sensing and GIS. Washington DC: ASPRS: 79–91

Lefsky M A, Harding D, Cohen W B, Parker G G and Shugart H H. 1999a. Surface lidar remote sensing of basal area and biomass in deciduous forests of eastern Maryland, USA. *Remote Sensing of Environment*, **67**(1): 83–98 DOI: 10.1016/S0034-4257-(98)00071-6

Lefsky M A, Cohen W B, Acker S A, Spies T A, Parker G G Spies T A and Harding D. 1999b. Lidar remote sensing of the canopy structure and biophysical properties of Douglas-fir western hemlock forests. *Remote Sensing of Environment*, **70**(3): 339–361 DOI: 10.1016/S0034-4257(99)00052-8

Lefsky M A, Cohen W B and Spies T A. 2001. An Evaluation of Alternate Remote Sensing Products for Forest Inventory, Monitoring, and Mapping of Douglas-fir Forests in Western Oregon. *Canadian Journal of Forest Research*, **31**(1): 78–87 DOI: 10.1139/x00-142

Lefsky M A, Cohen W B, Harding D J, Parker G G, Acker S A and Gower S T. 2002. Lidar remote sensing of aboveground biomass in three biomes. *Global Ecology and Biogeography*, **11**(5): 393–400 DOI: 10.1046/j.1466-822x.2002.00303.x

Lefsky M A, Harding D J, Keller M, Cohen W B, Carabajal C C, Espirito-Santo F D B, Hunter M O and de Oliveira R Jr. 2005. Estimates of forest canopy height and aboveground biomass using ICESat. *Geophysical Research Letters*, **32**(L22S02), DOI: 10.1029/2005GL023971

Luo Z M, Tian Q J and Hui F M. 2005. Retrieving leaf area indexes for coniferous forest in Xingguo county, Jiangxi province, in use of Landsat ETM+ images. *Journal of Nanjing University (Natural Sciences)*, **41**(3): 253–258

Means J E, Acker S A, Harding D J, Blair J B, Lefsky M A, Cohen W B, Harmon M E and McKee W A. 1999. Use of large-footprint scanning airborne lidar to estimate forest stand characteristics in the Western Cascades of Oregon. *Remote Sensing of Environment*, **67**(3): 298–308 DOI: 10.1016/S0034-4257-(98)00091-1

Nilson M. 1996. Estimation of tree heights and stand volume using an airborne lidar system. *Remote Sensing of Environment*, **56**(1): 1–7 DOI: 10.1016/0034-4257(95)00224-3

Pang Y, Li Z Y, Sun G Q, Lefsky M, Che X J and Cheng E X. 2007. Effects of terrain on the large footprint lidar waveform of forests. *Forest Research*, **20** (4): 464–468

Pang Y, Sun G Q and Li Z Y. 2006a. Large footprint lidar waveform modelling of forest spatial patterns. *Journal of Remote Sensing*, **10**(1):97– 103

Pang Y, Yu X F, Li Z Y, Sun G Q, Chen E X and Tan B X. 2006b. Waveform length extraction from ICEsat GLAS data and forest application analysis. *Scientia Silvae Sinicae*, **42**(7):137–140

Pang Y, Zhao F, Li Z Y, Zhou S F, Deng G, Liu Q W and Chen E X. 2008. Forest height inversion using airborne lidar technology. *Journal of Remote Sensing*, **12**(1):152–158

Sheng W T. 2001. A long-term study on development and succession of undergrowth vegetations in chinese fir (cunninghamia lanceolata) plantations with different density, *Forest Research*. **14**(5): 463–471

Sun G Q and Ranson K J. 2000. Modeling LIDAR returns from forest canopies. *IEEE Transactions on Geoscience and Remote Sensing*, **38**(6): 261–2626 DOI: 10.1109/36.885208

Sun G Q, Ranson K J, Kimes D S, Blair J B and Kovacs K. 2008. Forest vertical structure from GLAS: an evaluation using LVIS and SRTM data. *Remote Sensing of Environment*, **112**(1): 107–117 DOI: 10.1016/j.rse.2006.09.036

Yang J, Dong C H, Lu N M, Yang Z D, Shi J M, Zhang P, LiuY J and Cai B. 2009. FY-3A:the new generation polar-orbiting meteorological satellite of china. *Acta Meteorologica Sinica*, **67**(4): 501–509

Zhang H Q, Chen Y R and Niu D. 2004. Retrieving effective leaf area index of conifer forests using Landsat TM images in red soil hilly region. *Acta Agriculturae Universitis Jiangxiensis*, **26**(2): 159–163

Zhang R H. 1996. Model on Remote Sensing and the Basic Experiments. Beijing: Sciences press: 20–60

Zwally H J, Schutz B, Abdalati W, Abshire J, Bentley C, Brenner A, Bufton J, Dezio J, Hancock D, Harding D, Herring T, Minster B, Quinn K, Palm S, Spinhirne J and Thomas R. 2002. ICESat's laser measurements of polar ice, atmosphere, ocean, and land. *Journal of Geodynamics*, **34**(3–4): 405–445

中国南方森林冠顶高度Lidar反演
——以江西省为例

董立新[1,2]，李贵才[1,2]，唐世浩[1,2]

1. 中国遥感卫星辐射测量与定标重点开放实验室，北京 100081；
2. 国家卫星气象中心，北京 100081

摘　要：激光雷达(Lidar)与光学遥感的有效结合对中国南方区域森林冠顶高度反演意义重大，而国产卫星将为中国森林生态研究提供新的数据源。本文联合利用大脚印激光雷达GLA和国产MERSI数据，在实现GLAS波形数据处理和不同地形条件下森林冠顶高度反演算法基础上,建立了区域尺度不同森林类型林分冠顶高度GLAS+MERSI联合反演关系模型，进行了江西地区森林冠顶高度反演。总体上，GLAS激光雷达森林冠顶高度估算精度较高；且在与MERSI 250 m数据的联合反演模型中，针叶林模型精度较好(R^2=0.7325)；阔叶林次之(R^2=0.6095)；混交林较差(R^2=0.4068)。分析发现，考虑了光学遥感生物物理参数的GLAS+MERSI联合关系模型在区域森林冠顶高度估算中有较高精度，且在空间分布上与土地覆盖数据分布特征非常一致。

关键词：森林冠顶高度，星载激光雷达，GLAS，FY3A-MERSI

中图分类号：TP79　　**文献标志码：**A

引用格式：董立新，李贵才，唐世浩．2011．中国南方森林冠顶高度Lidar反演——以江西省为例．遥感学报，**15**(6): 1301–1314
Dong L X, Li G C and Tang S H. 2011. Inversion of forest canopy height in south of China by integrating GLAS and MERSI: The case of Jiangxi province in China. *Journal of Remote Sensing*, **15**(6): 1301–1314

1 引　言

森林垂直结构(高度、LAI等)与生物量是森林碳循环研究的敏感参数。传统地面测量方法在大尺度研究中有一定局限性，而激光雷达以其对森林垂直结构参数高精度的直接测量能力，在森林生态测量中越来越显示出不可比拟的优势。

近年来，国外许多研究者(Nilson，1996；Means等，1999；Lefsky 等，1997，1999a，1999b，2002，2005；Hudak 等，2002；Hyde 等，2005)发展了Lidar数据反演林木参数的反演算法，极大推进了Lidar在林业上的应用。美国马里兰大学与NASA-GSFC合作提出了星载植被激光雷达系统(Vegetation Canopy LIDAR，VCL)计划，在美国、加拿大和澳大利亚等多个国家进行实验，并对温带和热带森林的垂直结构和覆盖度进行了成功反演。Sun和Ranson(2000)将森林生长模型与Lidar波形模拟模型相结合表明Lidar波形数据很好地反映了森林的垂直结构。Lefsky等人(1997)提出了依赖人工方式检测地面回波的冠顶高度估算方法。Hyde等人 (2005)进一步提出了一种地面与冠顶高度自动检测策略，大大提高了激光雷达测量林木高度的应用前景。

国内的庞勇等人(2006a，2007)对星载记录完整波形数据的大光斑雷达系统进行了理论模拟；Sun等人(2008)对ICEsat GLAS的陆地与冠顶高度数据进行了评估。董立新(2008)改进地形指数法，提出了质心–地形指数法对坡度较大地区进行林分冠顶高度与生物量估算等研究。

Lidar数据是离散的，区域尺度的森林结构参数反演要联合栅格遥感数据。Lefsky等人(2001)等指出，尽管Lidar只是采样数据，但由于其有很高的测量精度，与其他栅格遥感数据联合使用将大大提高

收稿日期：2010-07-26；**修订日期：**2011-03-22
基金项目：国家重点基础研究发展计划(973计划)(编号: 2010CB950701-01，编号: CCSF-09-09)
第一作者简介：董立新(1973—　)，男，博士，副研究员，主要从事激光雷达及其应用研究。E-mail: dlx_water@163.com。

林业测量的精度。目前，将Lidar数据与光学遥感、多角度及微波遥感数据相结合，是区域尺度森林冠顶高度与生物量估算的有效方法(Sun和Ranson，2000；庞勇 等，2006b，2008；Dong 等，2009)。

以江西主要林区为实验区，于2009年10月进行了野外测量。对大脚印Lidar GLAS脚点波形数据进行处理，通过不同地形条件下森林冠顶高度反演算法得到研究区离散的森林冠顶高度，并联合使用MERSI 250 m光学遥感数据，建立了区域尺度森林冠顶高度GLAS+MERSI联合反演模型，制作了研究区森林冠顶高度图。

2 研究区和数据获取

2.1 研究区概况

研究区位于长江中下游南岸的江西省主要森林覆盖区，113°34′36″E—118°28′58″E，24°29′14″N—30°04′41″N之间，面积16.69万km^2，一般海拔300—600 m，最高海拔1918.3 m。

该地区属于中亚、亚热带森林生态系统，境内大小森林生态系统自然保护区有36个，面积共计213014 ha。主要有亚热、热带常绿阔叶林、温带落叶阔叶林，还有寒带特征的针叶林，混交林及灌木林等，多属天然次生，森林覆盖率已达60.05%。山地地区森林植被垂直分布明显，从低至高依次为毛竹林、常绿阔叶林、针阔叶混交林、针叶林、山顶苔藓矮林和山顶灌丛草甸等。地貌类型以山地和丘陵为主，山地占36%，丘陵占42%，平原岗地(含水域)占22%。

2.2 数据获取

2.2.1 激光雷达GLAS数据

GLAS是搭载于美国科学试验卫星ICEsat上的第一台星载Lidar传感器，能连续获取大气和地面回波数据。GLAS搭载有3个激光仪器，以91 d(每个33 d)重复轨道方案执行观测任务，在赤道附近相邻轨道间距为15 km，而在纬度80° 处，间距为2.5 km。为了最大限度的覆盖极地地区，在每一年中，选择不同时间段观测。激光光斑直径为60—70 m，光斑间隔为175 m(Brenner 等，2000)。GLAS由于具有较高的垂直分辨率，可提供重要的植被高度样点数据。其工作波段1064 nm回波数据提供的植被垂直结构信息将能更好地评价全球的植被分布和生物量(Zwally 等，2002)。

本文的GLAS数据为2008年的L3F的1064 nm GLA01回波波形数据与GLA14地理位置数据。研究区GLAS数据覆盖情况如图1所示，右下方为LAI试验样区及地基激光雷达实测样点布设图。

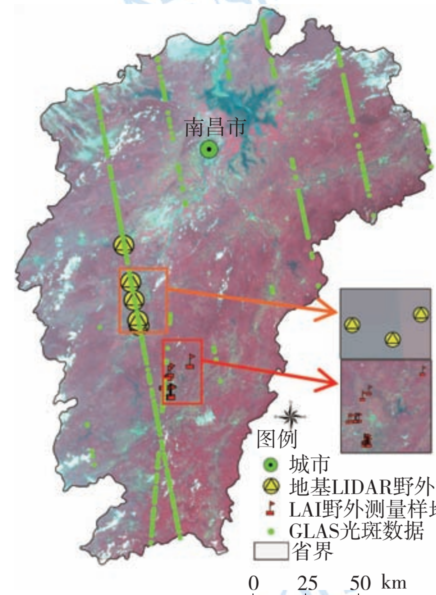

图 1 研究区FY3A/ERSI+GLAS数据及野外实验样区分布图

2.2.2 风云三号MERSI数据

新一代极轨气象卫星系列首发星风云3号A星(FY3A)，实现了全球全天候、三维、定量和多光谱遥感，以满足现代气象业务和全球变化遥感研究(杨军 等，2009)。FY3A携带了11台探测仪，其中，中分辨率光谱成象仪(MERSI)与MODIS 比较相似，星下点空间分辨率0.25—1.0 km。其中，250 m分辨率有5个通道，可提供可见光-近红外和中-远红外波段数据，主要探测云特性、植被、地面及表面温度等特征。

本文涉所用MERSI数据是0.47—0.865 um之间的B1—B4波段(图1)，获取时间为2009-08-29，晴朗少云(<2%)，数据经过地理精校正、云检测、大气校正及投影变换等预处理。

2.2.3 地面实验数据

选择江西中部地区地势平坦的5个GLAS脚点位置作为实验样区。考虑到仪器较重，携带不方便，选择距离道路较为便捷的样区实地测量，测量时在GLAS脚点70 m大小的范围内进行3个不同方位测量(如右小图)。在GLAS脚点位置，通过地基Lidar扫描仪Riegl LMS-Z360i实地测量获取Lidar点云数据，在

所带软件中提取树高最大值，验证GLAS森林冠顶高度算法精度。在一定的条件下，地面Lidar Riegl LMS-Z360i可扫描的半径范围可达到200 m，满足GLAS光斑的大小范围。

同时，沿其他GLAS脚点设置不同样区，各样区设置10 m×10 m大小样方3个，进行传统方法的林木参数测量，数据主要用于算法系数拟合。LAI数据为骆知萌等人(2005)在2003年对兴国县武夷山支脉粤山地段不同密度森林等级分布地区实测的LAI观测数据。研究使用的数字高程模型用于计算研究区坡度及地形指数参数。

3 森林冠顶高度模型构建

3.1 GLAS脚点林分冠顶高度算法

首先对每个GLAS激光脚点的回波波形数据进行处理(Sun 等，2008；董立新，2008；Duncanson 等， 2010)。处理算法主要包括：波形提取、高斯滤波、噪声估计、高斯回波分解与拟合、信号始末位置确定、地面回波位置确定与结果订正等步骤。

提取陆表有效回波后通过选用与激光发射脉冲宽度(4 ns)一致的高斯函数作滤波器(低通滤波)，实现平滑滤波。并采用直方图法(Sun 等，2008)对波形数据开始(Noisestart)和末尾阶段(Noiseend)信号的背景噪声进行估计，求取均值及方差等特征参数。最后应用Levenberg-Marquardt非线性拟合对波形数据进行有效拟合，并通过高斯回波分解，求取冠顶与地面等主要波峰位置(董立新，2008)(如图2)。

对接收的回波信号要通过反复实验，利用背景噪声特征对信号始、末位置进行确定(式(1)(2))。如果波形数据的值大于$threshold_{start}$，则为其开始位置；如果小于$threshold_{end}$，则为信号结束位置。

$$threshold_{start}=meanns_{start}+4\times sdevns_{start} \quad (1)$$

$$threshold_{end}=meanns_{end}+4\times sdevns_{end} \quad (2)$$

最后从信号结束位置开始逆向搜索，判断主要波峰位置与信号结束位置的间隔距离，如果大于激光脉冲的半宽则将其视为地面峰位置。

(1)平缓地区森林冠顶高度算法及校正

首先通过冠顶回波与地面回波位置，计算出回波距离(*Range*)。林分高度的计算是回波长度与记录间隔大小(*BinSize*)的乘积，即：

$$H=Range\times BinSize \quad (3)$$

为了克服在缓坡或粗糙度较大的情况下，地表回波出现的展宽及波峰初始位置的前展，需对树高(*H*)进行校正。校正方法采用Sun等人(2008)方法，即利用*SigEnd0*与*SigEnd*之间的距离差。校正后树高(H_t)为：

$$H_t=H-(SigEnd-SigEnd0) \quad (4)$$

由于坡度的影响，信号结束位置从*SigEnd0*扩展到了*SigEnd*，因此，*SigEnd0*表示此距离地面峰加上发射脉冲的半宽。

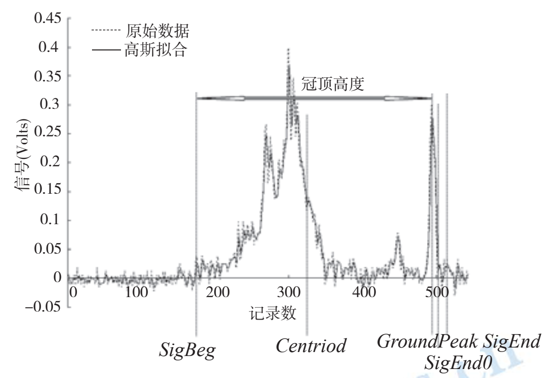

图 2 GLAS 波形参数与计算方法示意图

(2)坡度较大地区森林冠顶高度模型构建

坡度达到一定程度会对大脚印Lidar回波产生很大影响(Harding 等，1994；Heyder，2005)。因此，直接从波形数据中提取树高比较困难。Lefsky 等(2005)开发了“地形指数法”对坡度较大地区的森林冠顶高度进行反演。董立新(2008)对其进行改进并提出了“质心-地形指数法”，提高了坡度较大地区的森林冠顶高度反演精度。本文应用“质心-地形指数法”如下：

$$H=a_0(w_c-a_1\cdot g+a_2\cdot l) \quad (5)$$

式中，w_c为波形质心到回波信号结束位置的距离，质心位置在其波形面积的1/2处；g为地形指数，单位为m；l为波形边缘长度(*leading edge*)，单位为m；a_0、a_1和a_2分别为系数。

3.2 MERSI叶面积指数与覆盖度

以实验区MERSI数据植被指数(NDVI)作为自变量，以地面实测LAI为因变量，建立LAI-NDVI 间的关系模型：

$$\text{LAI}=a\times \ln(\text{NDVI})+b \quad (6)$$

覆盖度采用“像元二分模型”进行计算：

$$Fc=\frac{\text{NDVI}-\text{NDVI}_{min}}{\text{NDVI}_{max}-\text{NDVI}_{min}} \quad (7)$$

所得LAI和Fc结果经过验证可用于区域尺度森林冠顶高度反演。

3.3 GLAS与MERSI联合反演关系模型

在植被生长发育过程中，大部分叶面积与株高是同步增长的。因此，张仁华针对不同的作物类型与品种，提出了作物高度与覆盖度及叶面积指数的转换关系(张仁华，1996)：

$$H = A_H \frac{\mathrm{LAI}}{\mathrm{Fc}} \tag{8}$$

式中，H为作物高度，LAI为叶面积指数，Fc为覆盖度，A_H为特定系数。

在森林生态方面，传统生物量与LAI地面测量中的“异速生长法”便利用了植物单元各测量因子(如植株高度和茎直径等)与叶面积的变异关系。其基础理论认为茎和枝是支撑叶子的营养导管的集合(Chen 等，1997；Le Dantec 等，2000)。研究表明(姜凤岐和卢凤勇，1982；侯平 等，1994)，植株高度和冠幅直径能够更好地体现植被的结构特征，从而建立直观的叶面积指数与地上生物量估测模型。

因此，植株高度与LAI及覆盖度之间的相关性，能够为我们进行森林植被高度的空间外推提供可解释的生理生物意义及依据。

4 结果验证与分析

4.1 叶面积指数与覆盖度结果

根据LAI测量数据与MERSI-NDVI数据建立不同森林密度LAI-NDVI关系模型，如表1所示，较密林R^2达到0.8597；中等密度林(0.8 > 覆盖度 > 0.4)R^2达到0.6485；稀疏林R^2为0.3538。可见，两者具有一定的相关性，可进行LAI计算。从图3看出，在东南部和千烟洲中国科学院生态试验站及周围林区LAI较高，其他地区次之，其空间分布较为合理。

表1 不同森林密度LAI与MERSI—NDVI关系模型

森林密度	关系模型	R^2	样点数量
较密	LAI=5.4774 × ln(NDVI) + 6.8523	0.860	8
中等	LAI=2.1817 × ln (NDVI) + 3.1055	0.649	5
稀疏	LAI=1.9201 × ln (NDVI) + 2.7168	0.354	10

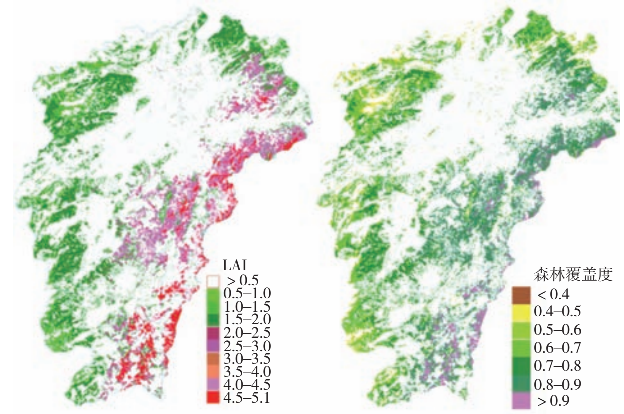

图3 森林叶面积指数与覆盖度分布图

不同密度森林叶面积指数的变化范围不同。统计分析MERSI反演的250 m LAI，发现针叶林变化范围是0.5—5.2，直方图统计发现96.11%在1—5.1之间。对比骆知萌等人(2003)及张红旗等人(2002)测量结果，与其变化范围在1.0—4.0之间基本一致。

我们将此结果扩展到1 km，与MODIS的LAI产品进行比较，两者在空间分布上基本一致，且大部分针叶林与阔叶林的LAI差值在 ± 1之间。混交林的差值较大，主要原因可能来自MODIS-LAI产品本身的误差及混交林LAI与NDVI关系较差所引起。

从森林覆盖度空间分布图上可以看出，计算结果与江西森林植被分布情况相一致。利用样点实地测量的森林覆盖度数据和MERSI反演结果对比分析，其拟和R^2达到0.8，样点误差在 ± 0.05左右。另外，与盛炜彤(2001)的测量结果对比分析，在江西省分宜县中国林科院亚热带林业实验中心上村林场样地的覆盖度(0.74)与MERSI反演结果(0.769)仅相差0.029。

总的来说，基于FY3A-MERSI的250 m森林叶面积指数与覆盖度结果较为满意，可用于本文的后续计算。

4.2 GLAS脚点林分冠顶高度结果验证

图4是研究区GLAS脚点的森林冠顶高度结果，结合森林分布图，可发现空间分布上冠顶高度较高的地区与研究区的森林分布呈现了很好的一致性：20 m高度的森林分布在东北、西北和南部生长年限较长的森林覆盖区，与该区域森林生物量较高相一致。而农田和草地等人类活动的中部地区的树高值较低。

为了对GLAS波形数据提取的森林冠顶高度进行精确验证，以减少目视估计所带来的误差，我们进行了“星-地”激光雷达森林冠顶高度对比分析(图5)。

从图5可以看出，除样区4由于坡度在20°—25°

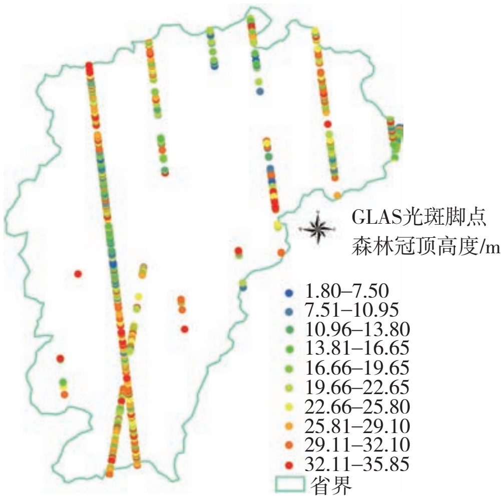

图 4 GLAS脚点森林冠顶高度图

之间，其结果与实测误差(与地基Lidar 结果误差1.78 m，与目视估测结果误差3.6 m)较大外，其他样区结果精度较高(小于1.2 m)。比较3种测量结果可以发现，GLAS星载Lidar测高体现了样区的最大高度，地基Lidar测高结果在样区不同样点的结果各不相同，传统目测也有此特点，但传统目测的结果误差较大，且结果精度不稳定。由于地基Lidar扫描仪比较重、体积大，在林区内大量多点测量比较困难，加之地基Lidar点云数据处理较为费时，因此此次试验只对与GLAS Lidar点地理位置精确匹配的林区进行测量。

总的来说，GLAS对森林冠层高度的测量结果比较满意，可以与LAI建立关系进行区域尺度森林冠顶高度联合反演。

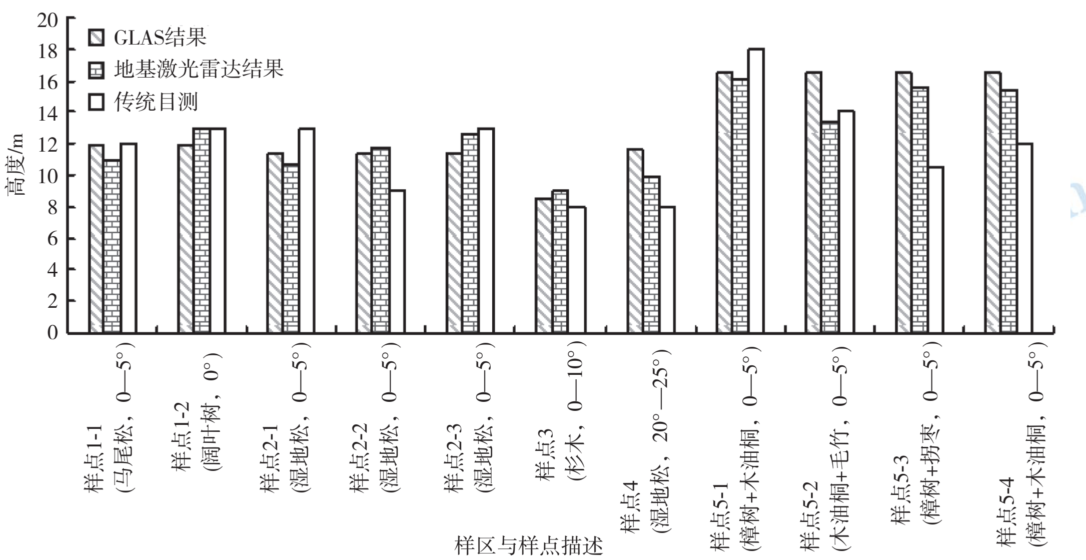

图 5 “星-地”激光雷达森林冠顶高度结果验证

4.3 GLAS与MERSI联合反演结果

利用式(8)建立了不同森林类型森林冠顶高度与LAI/Fc比值之间的关系模型(表2)。由于稀疏森林LAI-NDVI关系较差，不作建模。

表2 不同森林类型冠顶高度联合反演模型

森林类型/密度		关系模型	R^2	样点数量
针叶林	较密	$HEIGHT$=−595.9 × ln(LAI/Fc) + 989.44	0.792	5
	中等	$HEIGHT$=307.37 × ln(LAI/Fc) − 242.23	0.733	7
阔叶林	较密	$HEIGHT$=288.13 × ln(LAI/Fc) − 443.51	0.616	7
	中等	$HEIGHT$=22.494 × ln(LAI/Fc) + 7.3312	0.610	7
混交林	较密	$HEIGHT$=673.09 × ln(LAI/Fc) − 1064.1	0.413	39
	中等	$HEIGHT$=214.63 × ln(LAI/Fc) − 163.16	0.407	59

注：*HEIGHT*为激光雷达GLAS森林冠顶高度；LAI与Fc分别是MERSI反演叶面积指数与覆盖度

可见，针叶林类型的森林冠顶高度与LAI/Fc的关系比较好，两者拟合的R^2达到0.733以上；阔叶林次之，R^2达到0.610以上；做回归t检验，均达到极显著水平。混交林的关系较差，R^2仅为0.407。这可能与混交林LAI及覆盖度的生物物理特性有关。

利用以上不同森林类型的关系模型，结合森林类型覆盖图，对研究区的森林冠顶高度进行空间外推，图6中白色区域为非林区。

为了进一步对江西森林冠顶高度图结果进行精度评价，利用中科院通过人工目视解译由Landsat TM数据获得的土地覆盖结果作为参考，分析发现江西森林冠顶高度空间分布格局与土地类型高度一致，具体地，森林冠顶高度最高的区域分布在东南部武夷山支脉地区和各个主要森林保护区，井冈山和庐山地区森林冠顶高度也相对较高，这也与该区域森林生物量较

高相一致。该结果与GLAS脚点结果的空间分布基本一致，进一步的验证仍在继续。

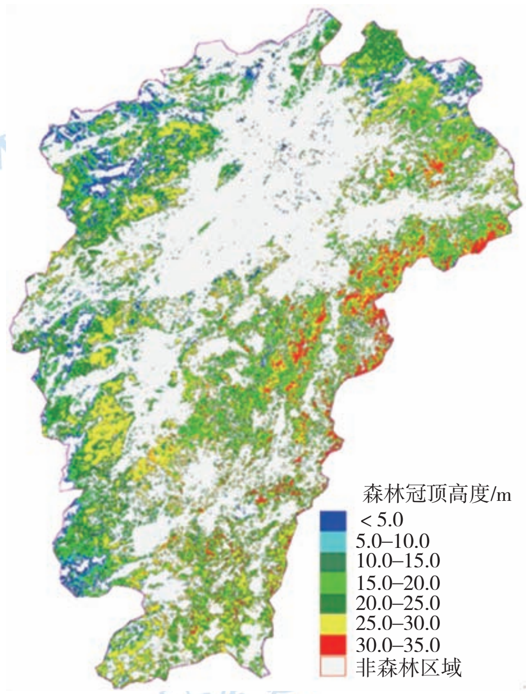

图 6 GLAS+MERSI联合反演森林冠顶高度图

5 结论与讨论

详述了大脚印激光雷达GLAS脚点波形数据处理和不同地形条件下森林冠顶高度的计算方法，并进行GLAS与FY3A-MERSI数据区域尺度森林冠顶高度联合反演研究。结果表明：

(1)由GLAS回波数据计算的波形参数及不同地形条件下森林冠顶高度具有较高的精度，“质心-地形指数法”估算中国南方地区坡度较大地区森林冠顶高度有较广的应用潜力；

(2)FY3A-MERSI数据的LAI计算方法虽然简单，但结果精度能够满足空间外推的需要，LAI/Fc比值与森林冠顶高度具有很好的相关性；且可获取性较容易，是比较理想的光学数据源。

(3)GLAS脚点的森林冠顶高度离散结果与MERSI联合反演区域尺度的森林冠顶高度在空间分布上基本一致，且与土地覆盖分布非常一致，从而可以更好地用于其他森林生物物理参数的定量反演。

志 谢 特别感谢中科院遥感应用研究所的黄华兵博士在地基激光雷达Riegl LMS-Z360i测量方面给与的指导和帮助。感谢一起参加江西地面激光雷达测量的实验队员：国家卫星气象中心王猛博士，中科院对地观测与数字地球科学中心程峰和唐福鑫两位博士。

REFERENCES

Brenner A C, Jay Zwally H,Bentley C R, Bea M C, David J H, Michelle A H, Minster J B, Lee Anne R, Saba J L, Thomas R H and Yi D H. 2000. Derivation of range and range distributions from laser pulse waveform analysis for surface elevations, roughness, slope, and vegetation heights. GLAS Algorithm Theoretical Basis Document Version 310

Chen J M, Rich P M, Gower S T, Norman J M and Plummer S. 1997. Leaf area index of boreal forests: theory, techniques and measurements. *Journal of Geophysical Research*, **102**(D24): 29429–29443

Dong L X. 2008. Estimation of the Forest Canopy Height and Above-ground Biomass Based on Multiplicatel Remote Sensing in Three Gorges. Beijing: Institute of Remote Sensing Applications Chinese Academy of Sciences (CAS): 56–98

Dong L X, Wu B F and Guo Z H. 2009. Estimation of forest canopy height by integrating multisensor data. *Proceedings of the SPIE*, **7471**: 74710H,. DOI: 10.1117/12.836304

Duncanson L I, Niemann K O and Wulder M A. 2010. Estimating forest canopy height and terrain relief from GLAS waveform metrics. *Remote Sensing of Environment*, **114**(1): 138–154

Harding D J, Bufton J L and Frawley J J. 1994. Satellite laser altimetry of terrestrial topography: vertical accuracy as a function of surface slope, roughness, and cloud cover. *IEEE Transactions on Geoscience and Remote Sensing*, **32**(2): 329-339 DOI: 10.1109/36.295048

Heyder U. 2005. Vertical Forest Structure from ICESat/GLAS Lidar Data. Mastors thesis Geography, VCL.12–50

Hou P, Yi L K and Yan C. 1994. Study on biomass of ammopipyanthus. *Arid Zone Research*, **11**(2): 16–18

Hudak A T, Lefsky M A, Cohen W B and Berterretche M. 2002. Integration of lidar and Landsat ETM+ data for estimating and mapping forest canopy height. *Remote Sensing of Environment*, **82**(2-3): 397–416 DOI: 10.1016/S0034-4257(02)00056-1

Hyde P, Dubayah R, Peterson B, Blair J B, Hofton M, Hunsaker C, Knox R and Walker W. 2005. Mapping forest structure for wildlife habitat analysis using waveform lidar: validation of montane ecosystems. *Remote Sensing of Environment*, **96**(3–4): 427–437 DOI: 10.1016/j.rse.2005.03.005

Jiang F Q and Lu F Y. 1982. The model of estimating above-ground biomass of caragana microphylla brush. *Acta Ecologica Sinica*, **2**(2):103–108

Le Dantec V, DufreÃne E and Saugier B. 2000. Interannual and spatial variation in maximum leaf area index of temperate deciduous stands. *Forest Ecology and Management*, **134**: 71–81 DOI: 10.1016/S0378-1127(99)00246-7

Lefsky M A, Cohen W B, Acker S A, Spies T A, Parker G G and Harding D. 1997. Lidar remote sensing of forest canopy structure and related bio-physical parameters at the H.J. Andrews experimental forest, Oregon, USA//Greer J D, ed. Natural Resources Management using Remote

Sensing and GIS. Washington DC: ASPRS: 79–91

Lefsky M A, Harding D, Cohen W B, Parker G G and Shugart H H. 1999a. Surface lidar remote sensing of basal area and biomass in deciduous forests of eastern Maryland, USA. *Remote Sensing of Environment*, **67**(1): 83–98 DOI: 10.1016/S0034-4257(98)00071-6

Lefsky M A, Cohen W B, Acker S A, Spies T A, Parker G G Spies T A and Harding D. 1999b. Lidar remote sensing of the canopy structure and biophysical properties of Douglas-fir western hemlock forests. *Remote Sensing of Environment*, **70**(3): 339–361 DOI: 10.1016/S0034-4257-(99)00052-8

Lefsky M A, Cohen W B and Spies T A. 2001. An Evaluation of Alternate Remote Sensing Products for Forest Inventory, Monitoring, and Mapping of Douglas-fir Forests in Western Oregon. *Canadian Journal of Forest Research*, **31**(1): 78–87 DOI: 10.1139/x00-142

Lefsky M A, Cohen W B, Harding D J, Parker G G, Acker S A and Gower S T. 2002. Lidar remote sensing of aboveground biomass in three biomes. *Global Ecology and Biogeography*, **11**(5): 393–400 DOI: 10.1046/j.1466-822x.2002.00303.x

Lefsky M A, Harding D J, Keller M, Cohen W B, Carabajal C C, Espirito-Santo F D B, Hunter M O and de Oliveira R Jr. 2005. Estimates of forest canopy height and aboveground biomass using ICESat. *Geophysical Research Letters*, **32**(L22S02), DOI: 10.1029/2005GL023971

Luo Z M, Tian Q J and Hui F M. 2005. Retrieving leaf area indexes for coniferous forest in Xingguo county, Jiangxi province, in use of Landsat ETM+ images. *Journal of Nanjing University* (*Natural Sciences*), **41**(3): 253–258

Means J E, Acker S A, Harding D J, Blair J B, Lefsky M A, Cohen W B, Harmon M E and McKee W A. 1999. Use of large-footprint scanning airborne lidar to estimate forest stand characteristics in the Western Cascades of Oregon. *Remote Sensing of Environment*, **67**(3): 298–308 DOI: 10.1016/S0034-4257(98)00091-1

Nilson M. 1996. Estimation of tree heights and stand volume using an airborne lidar system. *Remote Sensing of Environment*, **56**(1): 1–7 DOI: 10.1016/0034-4257(95)00224-3

Pang Y, Li Z Y, Sun G Q, Lefsky M, Che X J and Cheng E X. 2007. Effects of terrain on the large footprint lidar waveform of forests. *Forest Research*, **20** (4): 464–468

Pang Y, Sun G Q and Li Z Y. 2006a. Large footprint lidar waveform modelling of forest spatial patterns. *Journal of Remote Sensing*, **10**(1):97– 103

Pang Y, Yu X F, Li Z Y, Sun G Q, Chen E X and Tan B X. 2006b. Waveform length extraction from ICEsat GLAS data and forest application analysis. *Scientia Silvae Sinicae*, **42**(7):137–140

Pang Y, Zhao F, Li Z Y, Zhou S F, Deng G, Liu Q W and Chen E X. 2008. Forest height inversion using airborne lidar technology. *Journal of Remote Sensing*, **12**(1):152–158

Sheng W T. 2001. A long-term study on development and succession of undergrowth vegetations in chinese fir (cunninghamia lanceolata) plantations with different density, *Forest Research*. **14**(5): 463–471

Sun G Q and Ranson K J. 2000. Modeling LIDAR returns from forest canopies. *IEEE Transactions on Geoscience and Remote Sensing*, **38**(6): 261–2626 DOI: 10.1109/36.885208

Sun G Q, Ranson K J, Kimes D S, Blair J B and Kovacs K. 2008. Forest vertical structure from GLAS: an evaluation using LVIS and SRTM data. *Remote Sensing of Environment*, **112**(1): 107–117 DOI: 10.1016/j.rse.2006.09.036

Yang J, Dong C H, Lu N M, Yang Z D, Shi J M, Zhang P, LiuY J and Cai B. 2009. FY-3A:the new generation polar-orbiting meteorological satellite of china. *Acta Meteorologica Sinica*, **67**(4): 501–509

Zhang H Q, Chen Y R and Niu D. 2004. Retrieving effective leaf area index of conifer forests using Landsat TM images in red soil hilly region. *Acta Agriculturae Universitis Jiangxiensis*, **26**(2): 159–163

Zhang R H. 1996. Model on Remote Sensing and the Basic Experiments. Beijing: Sciences press: 20–60

Zwally H J, Schutz B, Abdalati W, Abshire J, Bentley C, Brenner A, Bufton J, Dezio J, Hancock D, Harding D, Herring T, Minster B, Quinn K, Palm S, Spinhirne J and Thomas R. 2002. ICESat's laser measurements of polar ice, atmosphere, ocean, and land. *Journal of Geodynamics*, **34**(3–4): 405–445

附中文参考文献

董立新. 2008. 基于多源遥感数据的三峡库区森林冠层高度与生物量估算方法研究. 北京：中国科学院遥感应用研究所

侯平，尹林克，严成. 1994. 沙冬青生物量研究. 干旱区研究，**11**(2): 16–18

姜凤歧，卢凤勇. 1982. 小叶锦鸡儿灌丛生物量的预测模型. 生态学报，(2): 103–108

骆知萌，田庆久，惠凤鸣. 2005. 用遥感技术计算森林叶面积指数—以江西省兴国县为例. 南京大学学报(自然科学)，**41**(3): 253–258

庞勇，李增元，Sun G Q，Lefsky M，车学俭，陈尔学. 2007. 地形对大光斑激光雷达森林回波影响研究. 林业科学研究，**20**(4): 464–468

庞勇，孙国清，李增元. 2006a. 林木空间格局对大光斑激光雷达波形的影响模拟. 遥感学报，**10**(1): 97–103

庞勇，于信芳，李增元，孙国清，陈尔学，谭炳香. 2006b. 星载激光雷达波形长度提取与林业应用潜力分析. 林业科学，**42**(7): 137–140

庞勇，赵峰，李增元，周淑芳，邓广，刘清旺，陈尔学. 2008. 机载激光雷达平均树高提取研究. 遥感学报，**12**(1): 152–158

盛炜彤. 2001. 不同密度杉木人工林林下植被发育与演替的定位研究. 林业科学研究，**14**(5): 463–471

杨军，董超华，卢乃锰，杨忠东，施进明，张鹏，刘玉洁，蔡斌. 2009. 中国新一代极轨气象卫星—风云三号. 气象学报，**67**(4): 501–509

张红旗，陈永瑞，牛栋. 2004. 红壤丘陵区针叶林有效叶面积指数遥感反演模型. 江西农业大学学报，**26**(2): 159–163

张仁华. 1996. 实验遥感模型及地面基础. 北京：科学出版社：20–60